

n-Butane Hydrogenolysis as a Probe of Surface Sites in Rhodium Metal Particles: Correlation with Single Crystals

D. Kalakkad,[†] S. L. Anderson,[†] A. D. Logan,^{†,§} J. Peña,^{†,⊥} E. J. Braunschweig,^{†,||} C. H. F. Peden,[‡] and A. K. Datye^{*,†}

Department of Chemical and Nuclear Engineering, University of New Mexico, Albuquerque, New Mexico 87131, and Sandia National Laboratories, Albuquerque, New Mexico 87185

Received: August 25, 1992; In Final Form: November 24, 1992

Rh metal was supported on alumina and silica supports and the particle size was varied (from <1 to >5 nm) by changing the metal loading from 0.03 to 7.2 μmol of Rh/ m^2 of support. Metal particle sizes were determined by transmission electron microscopy. Hydrogenolysis of *n*-butane was used as a probe reaction. The effect of particle size and preoxidation on the hydrogenolysis activity and product selectivity was studied. The ethane selectivity of the highly dispersed Rh was very different from that of the low index single crystal surfaces of Rh. As particle size was increased, the selectivity of the catalysts approached that of Rh(111). Annealing the catalysts at 773 K in H₂ led to better agreement between the supported Rh and single-crystal Rh(111). None of the catalysts after initial H₂ reduction resembled the (100) or (110) surfaces in their hydrogenolysis selectivity. Since the (111) close packed surface would be favored during particle growth, it is understandable that these high temperature treatments lead to better agreement between the behavior of small particles and single crystals.

Introduction

The catalytic behavior of small metal particles in a heterogeneous catalyst is known to vary with particle size, a phenomenon referred to as structure sensitivity.¹ These variations in activity and selectivity are believed to be caused by changes in the environment of surface atoms since they have fewer nearest neighbors as particle size is decreased. Indeed, in a classic paper by Van Hardeveld and Hartog,² it was shown that for small particles of closed polyhedral shape, the number of nearest neighbors varies in a systematic fashion with particle size. These authors calculated the statistics of surface atoms for a number of regular polyhedral particle shapes such as the octahedron or the cuboctahedron that are bounded by low index facets. For an octahedron of Rh, having a size smaller than 10 Å, the majority of surface atoms would have only seven nearest neighbors (C₇ atoms according to the nomenclature of Hardeveld and Hartog) whereas C₉ atoms would be the majority atoms on the surface of particles larger than 50 Å. Similar variations in the types of surface atoms would be expected in going from the fcc (110) surface to the fcc (111) surface. It would therefore be of interest to determine whether the catalytic behavior of small metal particles in a supported catalyst resembles the behavior of the corresponding single-crystal surfaces in the limit of small and large particles.

Such a study has been performed by Engstrom et al.,³ for *n*-butane hydrogenolysis over supported and single-crystal iridium. The selectivity patterns for the highly dispersed supported Ir closely resembled those for the Ir(110) (1 × 2) reconstructed surface. On the other hand, the close packed Ir(111) surface modeled very well the behavior of large Ir particles. The different product selectivity on the two single crystal surfaces was ascribed to differences in the reaction mechanisms operating on these single crystal surfaces. The (110) (1 × 2) surface has rows of surface atoms with only seven nearest neighbors and hence may provide coordinatively unsaturated surface atoms similar to those on highly dispersed Rh. The coordinatively unsaturated atoms on the (110)

(1 × 2) surface may allow the *n*-butane molecule to form a surface metallacycle intermediate which would lead to preferential ethane formation due to symmetrical cleavage. On the other hand, the formation of the metallacycle intermediate was thought to be sterically hindered on the atoms of the (111) surface, leading to statistical cleavage of *n*-butane.

In contrast to these results on Ir, the behavior of Rh metal surfaces was quite different,⁴ in that the hydrogenolysis selectivity of the (110) surface was unlike that of highly dispersed Rh reported in the literature.⁵ Comparison of the reactivity of supported Rh catalysts with that of metal single crystals is particularly interesting since it helps shed light on the nature of surface atoms in small metal particles. Recent work^{6,7} shows, for instance, that the equilibrium shape of fcc metal particles, such as Pt or Au, is almost nearly spherical and these particles have rather small (111) and (100) facets. On the other hand, in the catalysis literature,⁸ it has generally been assumed that the small particles in supported catalysts are polyhedral with rounded corners and bounded by low index metal facets. Our previous work on supported Pt⁹ confirmed the existence of faceted cubooctahedral particles, however, the catalytic probe reaction we used to measure reactivity, *n*-butane hydrogenolysis, was not very sensitive to exposed metal facets or to particle shape on the Pt catalysts.

On supported Rh, however, alkane hydrogenolysis has been shown to be a structure sensitive reaction. Yates and Sinfelt¹⁰ reported that ethane hydrogenolysis reactivity on supported Rh went through a maximum with increasing particle size. Particles having an average diameter of 12 Å were the most reactive. Yao et al.¹¹ found that both the selectivity and the activity for the hydrogenolysis of *n*-pentane over alumina supported rhodium was a function of particle size. Highly dispersed Rh was shown to selectively form ethane and propane due to selective cleavage of the central C-C bond, but on large particles the activity for this reaction sharply decreased, and the cleavage of *n*-pentane became nearly statistical. In this study we report the catalytic activity of supported Rh as a function of particle diameter. We contrast the catalytic behavior of the supported catalyst with that of Rh(111), Rh(110), and Rh(100) single crystals. The effect of oxidation-reduction cycling on catalyst activity has also been studied as a function of Rh metal particle size.

[†] University of New Mexico.

[‡] Sandia National Laboratories.

[§] Ford Motor Company, Dearborn, MI 48121.

[⊥] Dow Chemicals, Freeport, TX 77541.

^{||} 3M, St. Paul, MN 55144.

* To whom all correspondence should be addressed.

Experimental Section

The preparation of the Rh/silica catalyst was similar to that of Yates and Sinfelt.¹⁰ The support was CabOSil HS-5 fumed amorphous silica with a surface area of 300 m²/g. The Rh was loaded onto the support by aqueous impregnation of RhCl₃·xH₂O. The particle size was varied by increasing the metal loading. The Rh/Alumina samples were prepared according to the method used by Yao et al.¹¹ The alumina was Degussa AlonC with a surface area of 100 m²/g. The alumina is a mixture of γ and δ forms. The Rh precursor, Rh(NO₃)₃·xH₂O, was loaded by aqueous impregnation. The Rh/silica samples were pretreated in 20 std cm³/min (sccm) of flowing H₂ at 723 K, before the reactivity studies were performed. The Rh/alumina samples were first oxidized in 10% O₂ in He at 473 K, then reduced at 20 sccm H₂ at 573 K and subsequently passivated. Tables I and II provide characterization details for the samples used in this study. Two sets of samples with varying metal loading were prepared in order to establish the reproducibility of the measurements. Hydrogen chemisorption measurements were performed only on one of these sets, while all catalysts were examined by transmission electron microscopy (TEM). All of the samples were examined in a JEOL transmission electron microscope operated at 200 keV. The samples were supported on Cu grids. Average particle size and sample homogeneity was determined via elemental analysis performed using X-ray emission within the TEM. The purpose of TEM images was mainly to determine average particle diameter, and hence no micrographs are reported in this paper.

All flow reactor experiments were conducted in a 1/4-in. quartz differential reactor described elsewhere.¹² The flow rates for hydrogenolysis were 20 sccm of hydrogen and 1 sccm of *n*-butane. The hydrogen from Tri-Gas was 99.999% pure. The *n*-butane was from Matheson and 99.9% pure, with the two major impurities being isobutane and propane. Both gases were used without further purification. A Varian GC with a FID and packed column was used for on-line analysis of the reaction products. The high H₂/*n*-butane ratio ensured that there was negligible catalyst deactivation.

The UHV/microreactor system used in the single-crystal studies has been described by Logan et al.¹³ The ultrahigh-vacuum chamber was equipped with a UTI quadrupole mass spectrometer and a PHI cylindrical mirror analyzer for Auger electron spectroscopy. The microreactor was separated from the UHV chamber by an all-metal valve and the crystal was translated between the two chambers with retractable bellows. The microreactor was pumped by a 50 L/s Leybold/Hereaus turbo pump and the main chamber was pumped with a 220 L/s ion pump and a titanium sublimation pump. Base pressure in the system was 2 × 10⁻¹⁰ Torr. Surface composition was checked before and after reaction by Auger electron spectroscopy. The crystals were cleaned by repeated oxidation/vacuum annealing cycles. The crystal was oxidized at 923–973 K in 1 × 10⁻⁷ Torr of O₂ for 2–5 min. It was then annealed in 4 × 10⁻¹⁰ Torr by flashing to approximately 1250–1323 K.

All reactions on the single crystals were conducted at a hydrogen pressure of 200 and 10 Torr of *n*-butane. The crystal was resistively heated through two tungsten leads spot-welded to the back face. Reaction products were back-filled through an evacuated gas manifold to a stainless steel sampling bottle that was connected to the system through a Cajon VCR valve. The sampling bottle then was removed and connected to the sampling loop of the Varian GC for analysis. Due to the high H₂ overpressure, considerably less than a monolayer of carbon was deposited on the sample after reaction. We did not quantify the carbon due to overlap with the Rh peaks. However, the crystal was oxidized and annealed after every reaction to remove any surface carbon impurities.

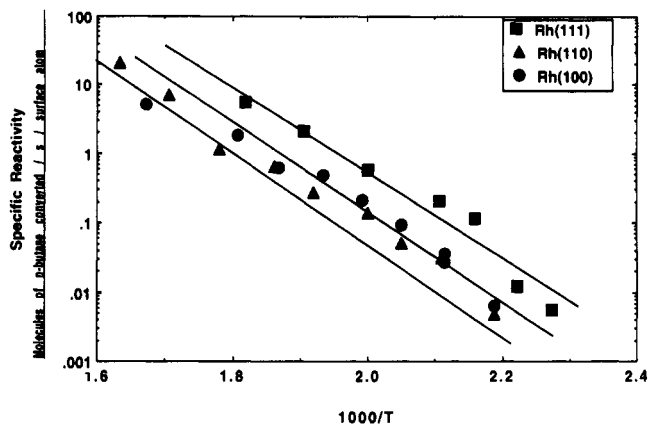


Figure 1. Hydrogenolysis activity on the Rh single crystals as a function of temperature (H₂ = 200 Torr; *n*-butane = 10 Torr).

TABLE I: Catalyst Characterization

	wt %	$\mu\text{mol}/\text{m}^2$	av particle diam (nm)
Alon C alumina, 100 m ² /g	0.15	0.15	nd
	0.63	0.63	nd
	2.2	2.2	1.0
	4.4	4.4	2.5
	7.2	7.2	3.0
Cabosil HS-5 silica, 300 m ² /g	0.1	0.035	nd
	0.3	0.1	nd
	0.5	0.17	nd
	1.0	0.35	2.0
	3.0	1.05	3.5
	5.0	1.7	4.5
	10.0	3.5	6.0

TABLE II: Catalyst Characterization

catalyst	Rh/SiO ₂ , 0.11 wt %	Rh/SiO ₂ , 3.4 wt %	Rh/Al ₂ O ₃ , 0.12 wt %	Rh/Al ₂ O ₃ , 8.4 wt %
<i>D</i> _{chemisorption} (Å)	16.15	21.86	12.26	31.72
<i>D</i> _{TEM, fresh} (Å)	n.d.	23.24	n.d.	18.83
<i>D</i> _{TEM, cycled} (Å)	n.d.	26.86	n.d.	21.01
H ₂ uptake ($\mu\text{mol}/\text{g}$ of catalyst)	6.62	156.48	9.51	282.78

Results

Single-Crystal Rh: Effect of Orientation. The hydrogenolysis activity on the Rh(111), Rh(110), and Rh(100) single-crystal surfaces is reported in Figure 1. The activity of the close packed (111) surface seems to be greater than that of the more open surfaces. Within the experimental error limits, the activation energy for the reaction on these surfaces seems very similar. However, the product distributions on these surfaces are markedly different as shown in Figure 2. The hydrocarbon selectivity is also affected by temperature. At low temperatures, cleavage of a single C–C bond occurs with the amounts of methane and propane formed being nearly equal. As temperature is increased, multiple hydrogenolysis occurs and eventually, methane becomes the dominant product. High methane selectivity is seen on all of the single-crystal surfaces at elevated temperatures, therefore it is only at low temperatures that the product distribution is sensitive to the nature of the exposed surface. The vertical line in Figure 2a–c marks the onset of multiple hydrogenolysis. As seen in Figure 2a, the (111) surface favors cleavage of the central bond in *n*-butane at low temperatures, yielding approximately 50% ethane from *n*-butane. The more open Rh surfaces (Figure 2b,c) cause nearly statistical cleavage of the C–C bond yielding approximately equal amounts of methane, ethane, and propane.

Supported Rh: Effect of Particle Size on Hydrogenolysis Selectivity. On supported catalysts, the experimentally accessible temperature range is limited because of the need to maintain conversion above about 0.1% to minimize experimental error and below 10% to ensure differential reactor operation. Such a

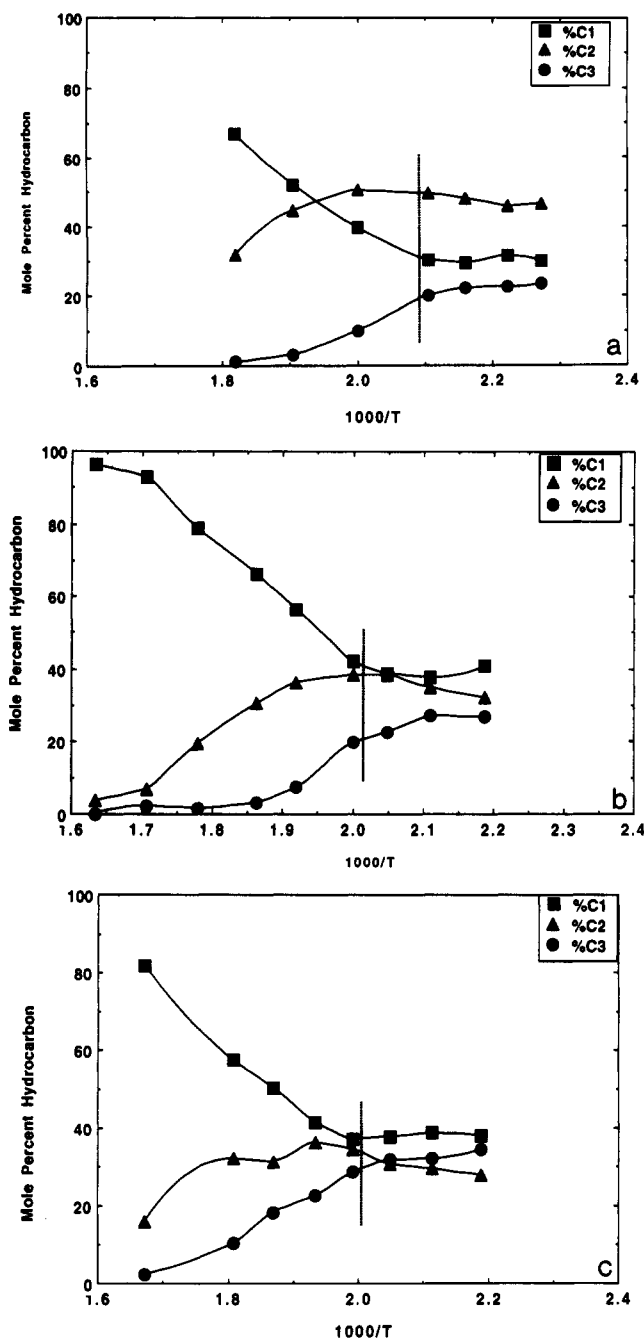


Figure 2. Hydrogenolysis product distributions on the Rh single-crystal surfaces (a) Rh(111); (b) Rh(110); (c) Rh(100) ($H_2 = 200$ Torr; n -butane = 10 Torr). The vertical line marks the onset of multiple hydrogenolysis wherein the amount of methane exceeds the amount of propane formed.

limitation is not encountered on the single crystals since reaction time can be varied to enable measurements of reaction rate over several orders of magnitude. The hydrogenolysis selectivity on the supported Rh catalysts is shown in Figures 3 and 4 over a rather limited range of temperatures. These data refer to the fresh state of the catalyst, which involves reduction at 723 K in flowing H_2 . All of these catalysts yield ethane as the major product with small but nearly equal amounts of methane and propane. At the higher temperatures used in activity measurements on the 0.1 wt % Rh catalysts, we see a decrease in percent ethane with increasing temperature. This change in selectivity is caused by the onset of multiple hydrogenolysis at temperatures above 473 K. Below 473 K, we see nearly equal amounts of the latter two products which confirms that cleavage of a single C-C bond occurs during the turnover of the butane. On the 4.4 wt % Rh/ Al_2O_3 and the 5.0 wt % Rh/ SiO_2 the product distribution is invariant with temperature since T is less than 473 K and we are

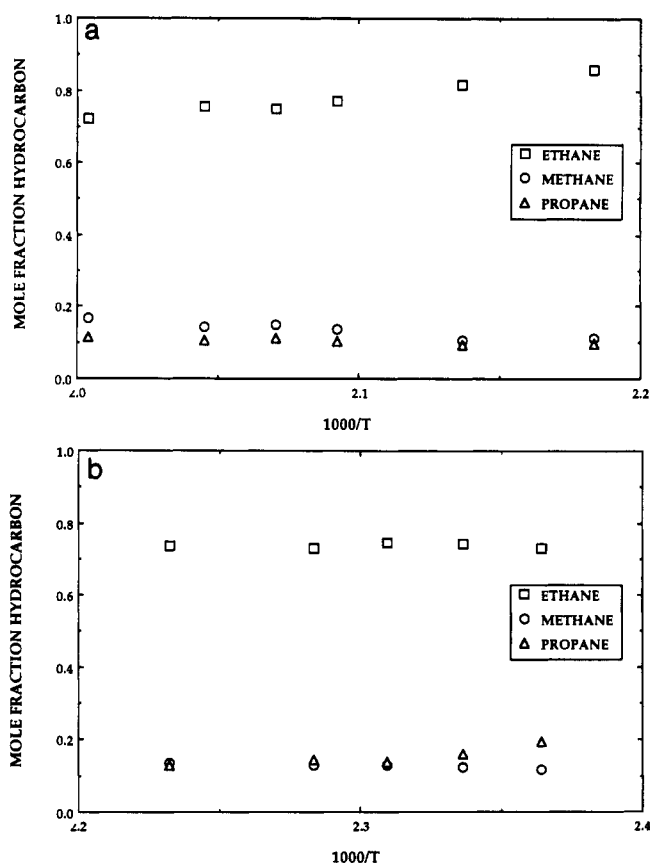


Figure 3. Hydrogenolysis product distributions over (a) 0.1 wt % Rh/ SiO_2 and (b) 5 wt % Rh/ SiO_2 ($P = 630$ Torr; H_2 : n -butane 20:1 sccm).

in the single-hydrogenolysis regime. In all subsequent figures, we report hydrogenolysis selectivity at 448 K to ensure that the data are obtained in the single-hydrogenolysis regime.

It is indeed surprising that despite the major differences in loading (and metal particle size), there is only a small difference in the ethane selectivity on the two catalysts whose behavior is reported in Figures 3 and 4. To provide a comparison with the Rh single crystals we have plotted in Figure 5 the ethane selectivity in the single hydrogenolysis regime as a function of nominal Rh metal loading in μmol of Rh/ m^2 of support. It is seen that as particle size is increased, the behavior of these catalysts approaches that of the (111) surface of Rh. It is surprising that none of the catalysts resemble the (110) or (100) surface in selectivity.

Supported Rh: Effect of Preoxidation on Activity and Selectivity. All of the catalysts whose ethane selectivity is shown in Figures 5a,b were subjected to oxidation-reduction cycles. Oxidation was performed in 10% O_2 in He at 773 K, following which the reaction mixture was introduced over the catalyst. The large excess of H_2 in the reacting mixture ensures that the catalyst is reduced quickly at a reaction temperature of 423–473 K. High-temperature reduction (HTR) involves reduction in flowing H_2 at 773 K. Figures 6 and 7 show the ethane selectivity at 448 K as a function of pretreatment for the silica- and alumina-supported catalysts. Catalysts having the lower metal loading do not cycle appreciably in their ethane selectivity whereas the higher metal loading catalysts show a selectivity similar to that of Rh(111) after HTR and a selectivity similar to that of Rh(110) or Rh(100) after preoxidation. The selectivity changes are most pronounced on the silica-supported catalysts, the alumina-supported catalysts seem to cycle much less in selectivity, even at the highest metal loading.

The drop in mole percent ethane after preoxidation is not caused by an increase in the extent of multiple hydrogenolysis. We find that the methane/propane ratio is unaffected by pretreatment and is between 1.1 and 1.2 both in the preoxidized and annealed

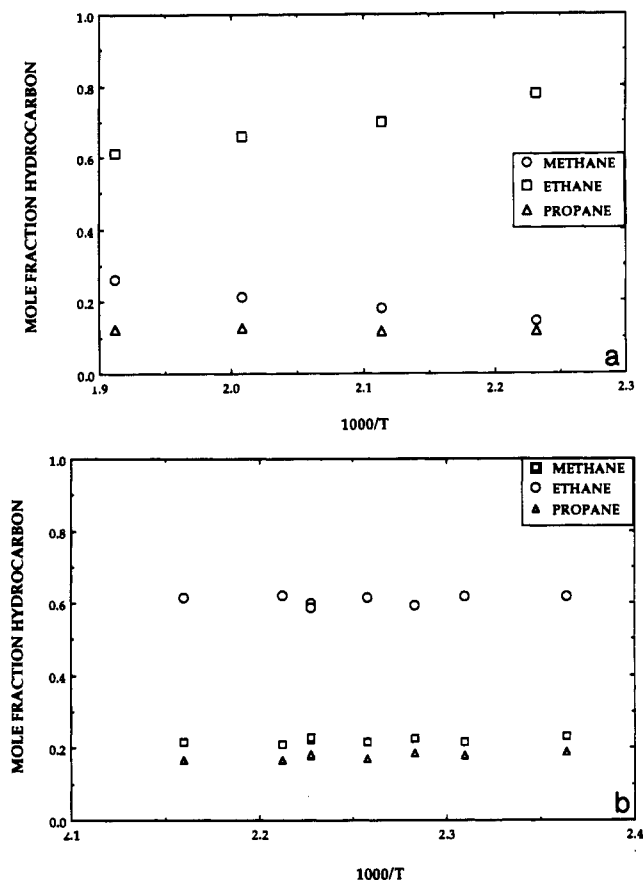


Figure 4. Hydrogenolysis product distributions over (a) 0.15 wt % Rh/Al₂O₃ and (b) 4.4 wt % Rh/Al₂O₃ ($P = 630$ Torr; H₂:*n*-butane 20:1 sccm).

states. Therefore, the drop in percent ethane must be due to a change in the active sites responsible for *n*-butane hydrogenolysis. Preoxidation and HTR also cause changes in catalyst activity. We present these reactivity changes by normalizing the activity after various pretreatments to the activity of the catalyst in its fresh state. Figure 8 shows the effect of pretreatment on the activity of Rh/SiO₂ and Figure 9 shows the effect on the Rh/Al₂O₃ catalysts. Once again, catalysts with low metal loadings do not cycle very much in activity. The higher metal loaded catalysts show an increase in activity due to preoxidation that is lost after high temperature reduction. The extent of activity cycling is less pronounced on the alumina-supported catalysts compared to the silica-supported ones.

Supported Rh: Effect of Particle Size on Activity. We have also examined the effect of loading and average particle size on catalyst activity. For the set of catalysts presented in Table I, no chemisorption measurements were performed. Consequently, to assess variations in specific activity, we have plotted the reactivity per m² of support as a function of metal loading. We would expect deviations from a straight line of slope unity if the specific activity on a given catalyst was very different from the others. Overall, the activity of these catalysts appears to scale linearly with the metal loading as shown in Figure 10. The activity starts to fall off from this linear behavior only at the highest metal loadings used in this study. This can be understood as being due to formation of larger metallic particles at these higher loadings. The deviation from linear behavior appears to occur only on catalysts where the metal particles are larger than 2.5 nm. Small Rh particles can be conclusively identified first at a metal loading of 1 wt % on silica and 2.2 wt % on alumina. However, the onset of particle detection should not be assumed to also represent onset of small particle formation. Particle detection on these high surface area supports is affected by background contrast from the support. These oxide supports

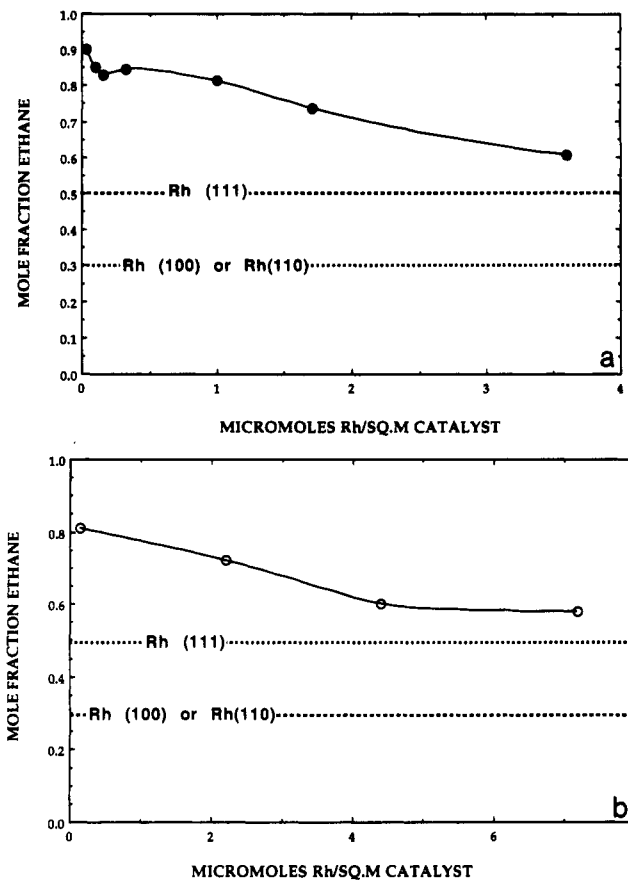


Figure 5. Ethane selectivity during *n*-butane hydrogenolysis as a function of metal loading (a) Rh/SiO₂ and (b) Rh/Al₂O₃ ($P = 630$ Torr; H₂:*n*-butane 20:1 sccm).

also tend to charge causing sample motion in the beam, and fuzzy images. It is likely that particles smaller than 10 Å are present on the low weight loading catalysts.

The previous sets of data were not corrected for chemisorption uptake and hence turnover frequencies (number of moles reacted per surface site per second) could not be derived. We have chemisorption uptakes available for most of the catalysts reported in Table II. The turnover frequencies for a 0.1 and 3.5 wt % Rh/SiO₂ and a 0.14 wt % Rh/Al₂O₃ are presented in Figures 11 and 12, respectively. We find that the activation energy as well as the turnover frequency do not appear to depend on metal loading or support. It is also seen that the TOF on the fresh catalyst agrees with that in the HTR state and it is preoxidation that leads to an increase in activity. The specific activity in the preoxidized state has not been corrected for any increase in metal surface area.

Discussion

Hydrogenolysis Selectivity of the Single Crystals. We first compare hydrogenolysis selectivity of the Rh single-crystal surfaces with that of the supported metal catalysts. In view of the temperature dependence of hydrogenolysis selectivity, all comparisons of selectivity are done at low temperatures where single hydrogenolysis of a C-C bond occurs. We find that the Rh(111) surface favors cleavage of the central bond in ethane leading ≈50% ethane during *n*-butane hydrogenolysis. During *n*-pentane hydrogenolysis, Rh(111) was also shown to favor central bond scission causing the amount of ethane + propane to exceed that of methane + butane. In contrast, Engstrom et al.³ observed nearly statistical cleavage of C-C bonds during *n*-butane hydrogenolysis on Ir(111).

On the more open Rh surfaces, Rh(110) and Rh(100), we find nearly statistical cleavage of C-C bonds from *n*-butane. Likewise,

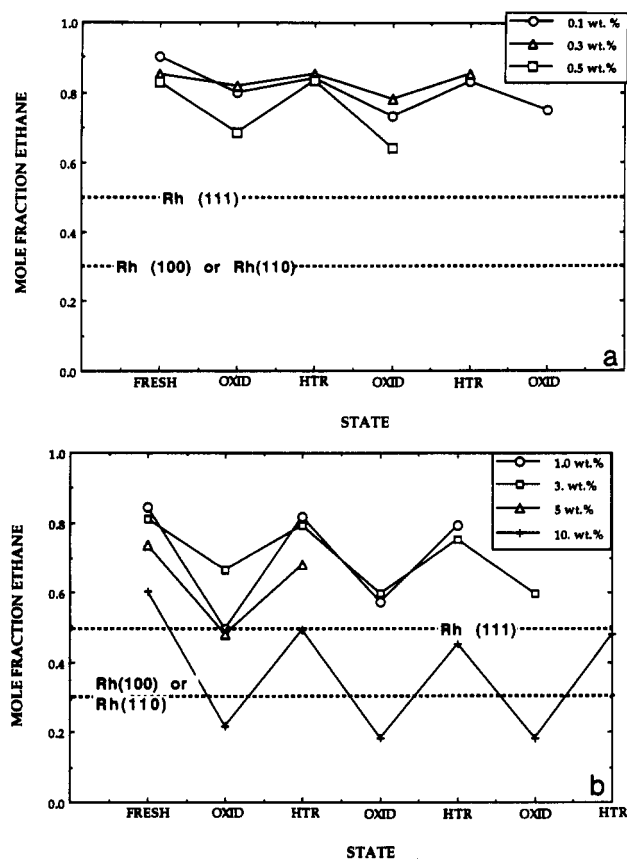


Figure 6. Effect of pretreatment on ethane selectivity during *n*-butane hydrogenolysis over silica supported catalysts (a) having $< 1\text{ wt. \%}$ Rh and (b) having $\ge 1\text{ wt. \%}$ Rh ($P = 630\text{ Torr}$; H_2 :*n*-butane 20:1 sccm).

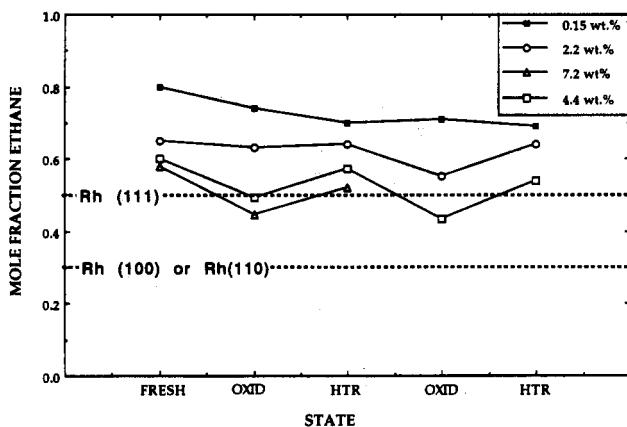


Figure 7. Effect of pretreatment on ethane selectivity over alumina-supported catalysts ($P = 630\text{ Torr}$; H_2 :*n*-butane 20:1 sccm).

during *n*-pentane hydrogenolysis, Logan et al.¹³ observed nearly statistical cleavage of C-C bonds. The behavior of Ir(110) was very different where a high selectivity to central bond scission was found. This unusual selectivity was related to occurrence of the missing row reconstruction on the Ir(110)-(1 × 2) surface, that leads to coordinatively unsaturated C_7 atoms on this surface. On Rh(110) where such a reconstruction does not occur, we find behavior very similar to Rh(100).

Effect of Particle Size and Pretreatment on Selectivity. The hydrocarbon selectivity of highly dispersed Rh is very different from that of any of the single-crystal surfaces we have examined. We find a high selectivity to formation of ethane ($\approx 80\%$) on highly dispersed Rh and as metal loading is increased, there is a drop in ethane selectivity to $\approx 60\%$. There is no particular particle size at which the hydrocarbon selectivity of the fresh catalyst resembles that of Rh(110) or Rh(100). On the basis of TEM observations, we conclude that the larger metal particles

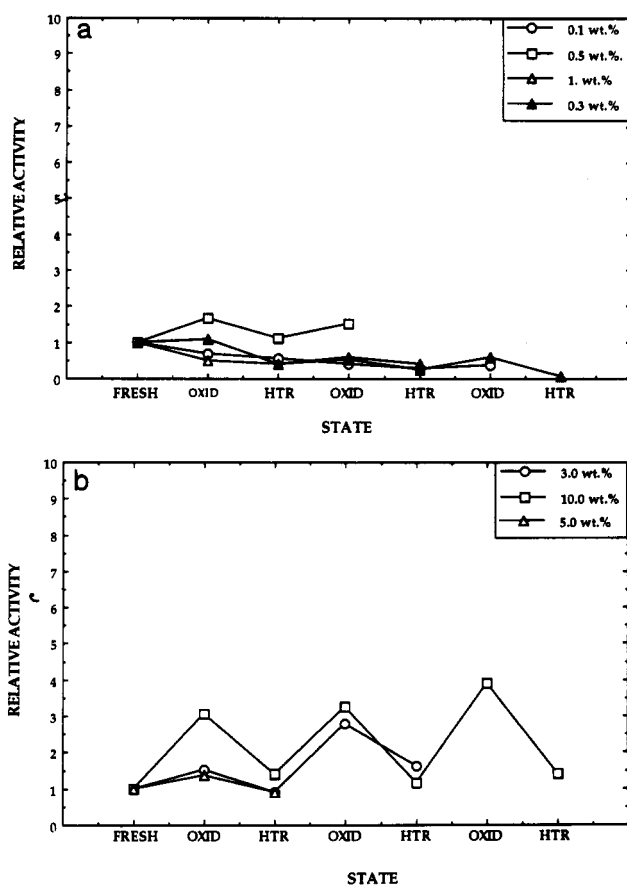


Figure 8. Relative activity as function of pretreatment on Rh/SiO_2 catalysts (a) having $\le 1\text{ wt. \%}$ Rh and (b) having $> 1\text{ wt. \%}$ Rh wherein relative activity is defined as the activity normalized to the activity of the catalyst in its fresh state.

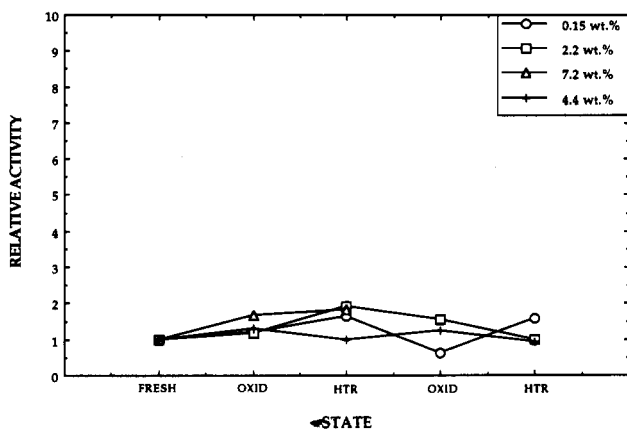


Figure 9. Relative activity as function of pretreatment on $\text{Rh/Al}_2\text{O}_3$.

after H_2 reduction are distorted cubooctahedra exposing prominent (111) facets.¹⁴ The types of surface atoms in a cubooctahedron of Rh are presented in Figure 13 using the equations presented by Van Hardeveld and Hartog.² It is clear that as the particle size grows larger, the majority of surface atoms become more (111)-like. On the other hand, as particle size decreases, the number of edge atoms start to increase in proportion, but these edge and corner atoms (despite being C_7 atoms) have quite different environments than the C_7 atoms on an unreconstructed Rh(110) surface. Figure 14 shows schematically the surface atoms on a (110) surface, on a reconstructed (110) surface and an edge atom on a cubooctahedron. If the ethane selectivity on the highly dispersed Rh is due to a metallacycle intermediate, it is reasonable to assume that formation of such an intermediate would be sterically hindered on Rh(110) due to the presence of neighboring C_7 atoms which would not be present on the (110)-

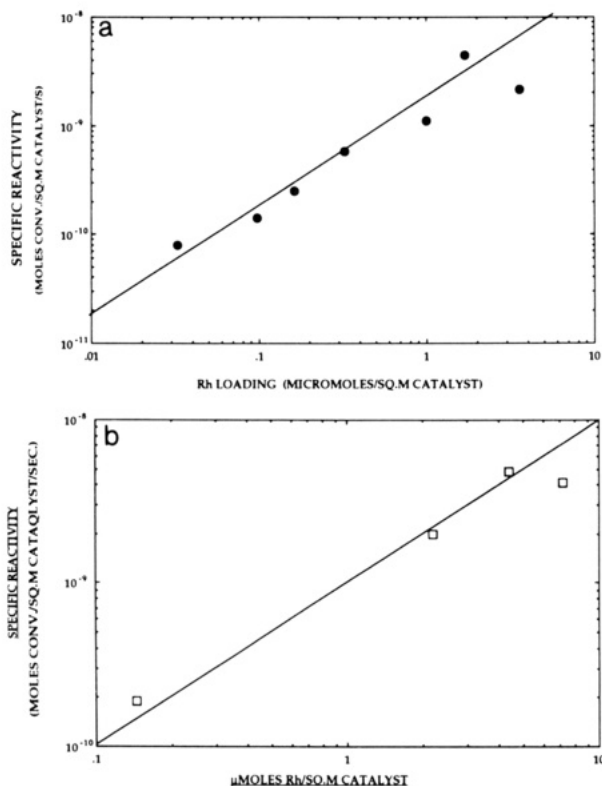


Figure 10. Hydrogenolysis activity as a function of metal loading (a) silica and (b) alumina.

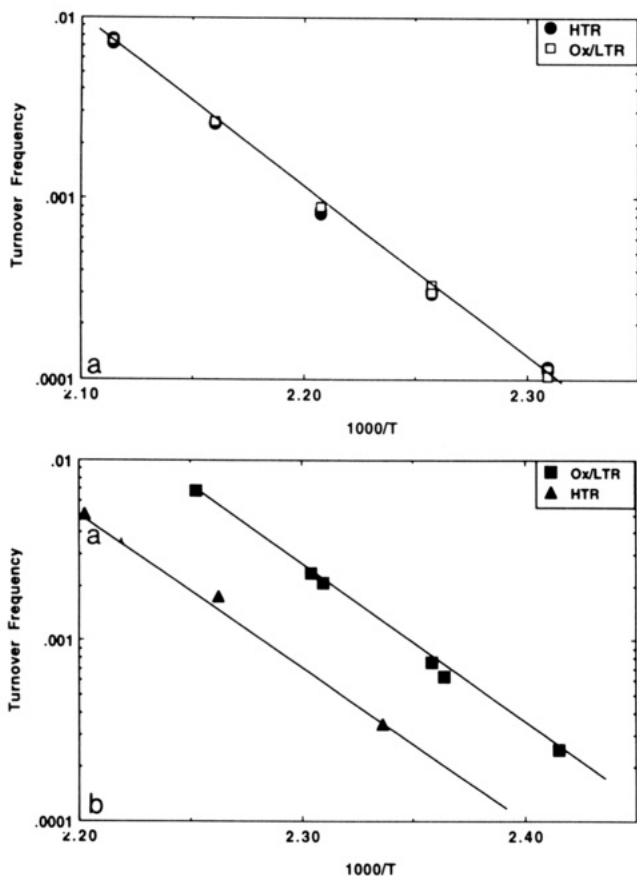


Figure 11. Turnover frequency for n-butane hydrogenolysis on Rh/SiO₂ (a) 0.1 wt % Rh and (b) 3.5 wt % Rh ($P = 630$ Torr; H₂:n-butane 20:1 sccm).

(1 × 2) surface or a corner atom in a cubooctahedron. Consequently, we conclude that while the (111) surface is a good model for large metal particles, the small particles cannot be

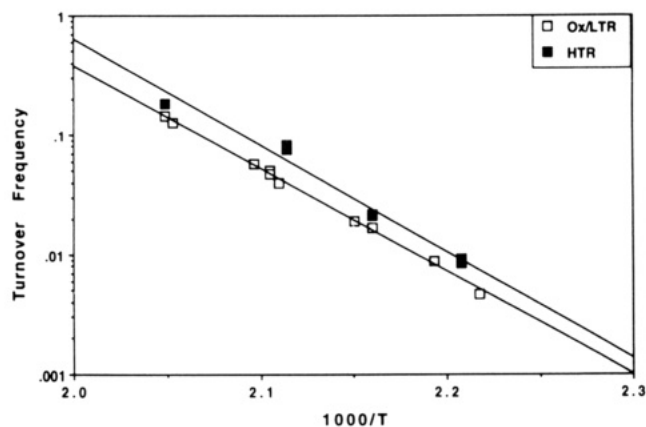


Figure 12. Turnover frequency for n-butane hydrogenolysis on Rh/Al₂O₃, 0.14 wt % Rh.

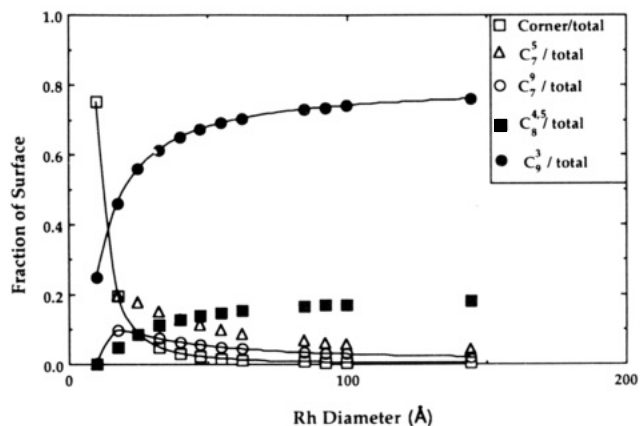


Figure 13. Statistics of surface atoms for a Rh cubooctahedron, based on the equations presented in ref 2.

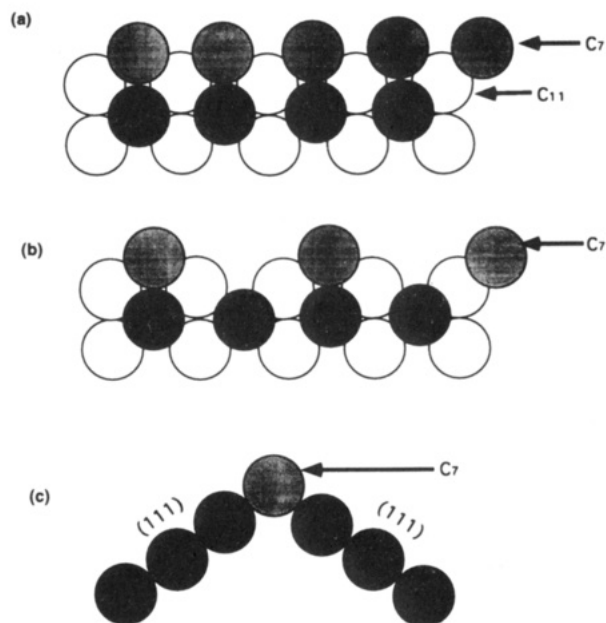


Figure 14. Representation of C₇ atoms on (a) fcc (110) surface, (b) fcc (110)-(1 × 2) surface, and (c) edge atoms in a cubooctahedron.

modeled by the (110) or the (100) surfaces, at least in the case of Rh metal.

Preoxidation of the catalyst causes a distinct change in hydrocarbon selectivity which also helps to distinguish the Rh catalysts having a low metal loading (no particles discernible by TEM) from that of Rh catalysts having a higher metal loading. Preoxidation of catalysts containing metal particles >4 nm causes a decrease in ethane selectivity such that the selectivity approaches

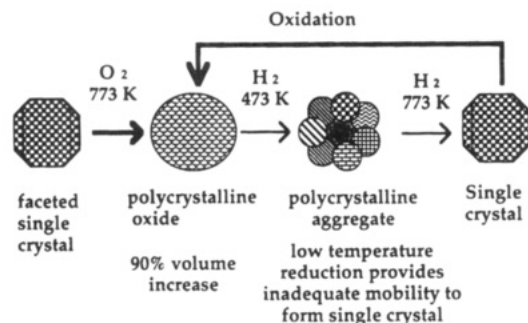


Figure 15. Schematic diagram showing how surface structure changes are caused by oxidation–reduction cycling of Rh metal particles.

that of Rh(110) or Rh(100). On the other hand, HTR causes an increase in ethane selectivity causing the behavior to approach that of Rh(111). Similar changes in hydrocarbon selectivity have been reported previously by us¹⁵ as well as other researchers.¹⁶ Observations of particle microstructure suggest that preoxidation causes a roughening of the surface according to the model shown schematically in Figure 15. Experimental verification is provided by transmission electron micrographs.¹⁷

The driving force for these surface structure changes is the volume increase upon oxidation of the metal. The oxidation of Rh transforms single-crystal particles into polycrystalline oxide particles which are very easy to reduce. Reduction in H₂ can occur at temperatures as low as 323 K.¹⁴ At such low temperatures, the mobility of metal atoms would be quite low, thereby leading to formation of polycrystalline metal aggregates with rather rough surfaces. Annealing in H₂ at 773 K tends to transform the polycrystalline aggregates back into single crystals that expose pronounced (111) facets. Our results therefore show that the surface structure of a metal particle can reversibly change from a close-packed (111)-like surface to a rougher (100) or (110)-like surface. We have confirmed that after reaction, there is no surface oxygen detectable by AES on the preoxidized Rh surface.¹³ Therefore, the altered hydrogenolysis selectivity must be related to morphological changes in the metal surface. These changes in morphology also occur on single crystal Rh(111) confirming that the oxide support plays a very minimal role in mediating these surface structure changes.

Our experimental observations suggest that changes in hydrocarbon selectivity due to pretreatment are more pronounced on Rh catalysts having a higher metal loading, very little change in selectivity being seen on catalysts having a low metal loading. We suspect that this is simply a particle size effect. Since the process of oxidative restructuring involves transformation of a single crystal into a polycrystalline aggregate, there must be a critical size below which there are simply not enough atoms present to permit transformation of a single crystal into a polycrystalline particle. We attempted to determine this critical size by preparing catalysts with increasing metal loading, hoping to find catalysts that cycle in activity and others that do not. As seen in Figure 6, catalysts having a metal loading below 1 wt % Rh/silica, where metal particles are not readily detectable by TEM, do not cycle appreciably in hydrocarbon selectivity. A conservative estimate of this minimum detectable size would be 10 Å, and these are the particles whose selectivity is unaffected by oxidation–reduction cycling. As weight loading is increased over 1 wt %, we start to see identifiable metal particles in the TEM and a gradual increase in the extent of selectivity cycling due to preoxidation. There is, however, a distribution of particle sizes which may account for the gradual onset of selectivity cycling. The catalyst selectivity is an arithmetic average of the behavior of small particles (whose properties are not affected by preoxidation) and large particles (which yield between 30% and 50% ethane).

Effect of Particle Size on Catalyst Activity. The results presented here suggest that we are dealing with two types of Rh

species on the oxide support: highly dispersed Rh particles (<10 Å) whose behavior is not affected by preoxidation, and metallic particles that can be seen in the TEM and whose ethane selectivity varies between 30% in the preoxidized state and 50% after annealing in H₂. The overall catalyst behavior represents an average of the selectivity of two kinds of Rh weighted by the relative amounts of the two types of Rh species. However, the weighting will be affected by the specific activity of the two kinds of Rh species. It is possible that the highly dispersed Rh may be much more reactive than metallic Rh, as has been suggested in the case of ethane hydrogenolysis on Rh.¹⁰ To investigate this aspect, we plotted the effect of metal loading on *n*-butane hydrogenolysis activity in Figure 10. The loading is expressed in terms of μmol of Rh/m² of support so that the behavior of the silica and alumina supports can be contrasted.

We find that activity per m² of support catalysts scales linearly with increasing metal loading. Deviations from linearity occur only on catalysts where particles larger than 2.5 nm were seen. These deviations would be consistent with the drop in percent metal exposed with increasing loading. However, there are two anomalous points on both supports where activity seems to increase over that expected based on this linear scaling relationship. These catalysts (the 5 wt % Rh/SiO₂ and 4.4 wt. % Rh/alumina) also do not appear to be affected by preoxidation as much as the catalysts with higher or lower loading. It is possible that these catalysts are better dispersed than the ones immediately on their right or left in terms of metal loading. The increase in activity can only be explained by an increase in turnover frequency which has not yet been determined on these samples. However, chemisorption uptakes and turnover frequencies are available on the set of samples reported in Table II. As shown in Figure 11, there is no difference between the turnover frequency and activation energy when the highly dispersed Rh sample is compared with a higher loaded sample that contains metallic particles. The turnover frequencies in Figure 11 do not agree with those obtained from the Rh single crystals since the operating conditions were quite different, a flow reactor being used for the supported catalysts whereas a batch reactor was used for the single crystal work. The partial pressures of H₂ and *n*-butane were 600 Torr of H₂ and 30 Torr of *n*-butane for the flow reactor study compared with 200 and 10 Torr for the single crystals. However, in a previous study,¹³ we compared the reactivity of Rh(111) with an annealed Rh/SiO₂ using identical conditions and found that the reactivities were in very good agreement.

Preoxidation also causes an increase in the activity of the Rh catalysts, but only on those catalysts that contain metallic particles. The activity cycling is less pronounced on the alumina supported Rh. The extent of activity cycling appears to correlate with the extent of selectivity cycling. The increase in activity is caused in part by the roughening of the surface as depicted in the schematic model in Figure 15, and in part due to a change in the intrinsic activity of the rougher surface. Systematic changes in activity are not seen when comparing Rh(111) with the rougher Rh single crystal surfaces. However, the effect of preoxidation was also seen in the case of *n*-pentane hydrogenolysis on preoxidized Rh single crystals. In the latter instance, the increased activity also led to a complete change in the hydrocarbon cleavage patterns with a loss of selectivity due to multiple hydrogenolysis. We do not see onset of multiple hydrogenolysis in this study and correspondingly see less of an enhancement in activity due to preoxidation. The factor of 4 increase cannot be explained by an increase in metal surface area as measured by H₂ chemisorption, which is generally around 30%. We do not see any break up of Rh particles as seen by Gao and Schmidt¹⁶ who saw increase in metal surface area of 3–4 times. At present, we cannot explain the 4-fold increase in catalyst activity except to suggest that the rougher Rh surfaces created by preoxidation are more reactive.

A similar increase in activity was seen on supported Ru for water gas shift catalysis by Taylor et al.¹⁸ when the catalyst was preoxidized.

Summary and Conclusions

We have shown that the *n*-butane hydrogenolysis selectivity is sensitive to the nature of the Rh single crystal surface exposed. Rh(111) favors cleavage of the central bond to yield 50% ethane while the Rh(110) and Rh(100) yield statistical cleavage of carbon bonds and approximately 30% ethane in the hydrocarbon products. Highly dispersed Rh is very different from any of these single crystals in terms of its hydrogenolysis selectivity, yielding approximately 80% ethane in the products. As Rh particle size is increased, hydrogenolysis selectivity approaches that of Rh(111). Preoxidation of the supported Rh at 773 K causes the ethane selectivity to drop to near 30% and a corresponding increase in hydrogenolysis activity of approximately 4 times. The increased activity and altered hydrogenolysis selectivity can be restored by annealing in H₂ at 773 K. These changes in activity and selectivity are reversible and are caused by surface restructuring that occurs on the Rh surfaces due to volume increase upon oxidation and formation of rough surfaces when the catalyst is reduced under mild conditions. Such changes in activity and selectivity are not seen on small Rh particles, presumably because the small size does not permit transformation of a single crystal into a polycrystalline aggregate. When Rh catalysts of increasing particle size are prepared by increasing the metal loading, we would expect to first form small clusters till we saturate the number of sites that lead to nucleation of Rh. Increasing loading will cause larger particles to form, resulting in a distribution in metal particle size. Therefore attempts to correlate catalyst behavior with particle size are complicated by the possible existence of a dispersed and metallic component. When the catalyst is heated at elevated temperatures, the dispersed phase may transform into the metallic phase. Such complications make it difficult to

correlate catalytic behavior with particle size. Our results suggest that the Rh particles do expose a (111)-like surface with increasing particle diameter, which would be consistent with a near-cubooctahedral shape for these particles.

Acknowledgment. Financial support from the Petroleum Research Fund, administered by the American Chemical Society, and from Mobil R & D is gratefully acknowledged. Transmission electron microscopy was performed at the Microbeam analysis facility within the department of Geology at the University of New Mexico.

References and Notes

- (1) Boudart, M. *Adv. Catal. Rel. Subj.* **1969**, *20*, 153.
- (2) Van Hardeveld, R.; Hartog, F. *Surf. Sci.* **1969**, *15*, 189.
- (3) Engstrom, J. R.; Goodman, D. W.; Weinberg, W. H. *J. Am. Chem. Soc.* **1986**, *108*, 4653.
- (4) Datye, A. K.; Hegarty, B. F.; Goodman, D. W. *Farad. Discuss. Chem. Soc.* **1989**, 87.
- (5) Wong, T. C.; Chang, L. C.; Haller, G. L.; Oliver, J. A.; Scaife, N. R.; Kamball, C. J. *Catal.* **1984**, *87*, 389.
- (6) Metois, J. J.; Heyraud, J. C. *J. Cryst. Growth* **1980**, *50*, 571.
- (7) Lee, W. H.; Van Loon, K. R.; Petrova, V.; Woodhouse, J. B.; Loxton, C. M.; Masel, R. I. *J. Catal.* **1989**, *120*, 421.
- (8) Anderson, J. R. *Structure of Metallic Catalysis*; Academic Press: New York, 1975; p 253.
- (9) Ramachandran, A.; Anderson, S. L.; Datye, A. K. *Ultramicroscopy*, in press.
- (10) Yates, D. J. C.; Sinfelt, J. H. *J. Catal.* **1967**, *8*, 348.
- (11) Yao, H. C.; Yao, Y. F. Y.; Otto, K. *J. Catal.* **1979**, *56*, 21.
- (12) Blankenburg, K.; Datye, A. K. *J. Catal.* **1991**, *128*, 1.
- (13) Logan, A. D.; Sharoudi, K. A.; Datye, A. K. *J. Phys. Chem.* **1991**, *95*, 5568.
- (14) Logan, A. D.; Braunschweig, E. J.; Datye, A. K.; Smith, D. J. *Ultramicroscopy* **1989**, *31*, 132.
- (15) Braunschweig, E. J.; Chakraborti, S.; Logan, A. D.; Datye, A. K. *Proc. 9th Intl. Congr. Catal.* Phillips, M. J.; Ternan, M., Eds.; The Chemical Institute of Canada, 1988, Vol. III, p 1122.
- (16) Gao, S.; Schmidt, L. D. *J. Catal.* **1988**, *111*, 210.
- (17) Chakraborti, S.; Datye, A. K.; Long, N. J. *J. Catal.* **1987**, *108*, 444.
- (18) Taylor, K. C.; Sinkewitch, R. M.; Klimish, R. L. *J. Catal.* **1974**, *35*, 34.